# Influence of adjacent metal films on magnon propagation in $Y_3Fe_5O_{12}$

Sotaro Mae,* Ryo Oshshima,*,† Ei Shigematsu, Yuichiro Ando, Teruya Shinjo, and Masashi Shiraishi
*Department of Electronic Science and Engineering, Kyoto University, Nishikyo-ku, Kyoto 615–8510, Japan*

(Received 15 October 2021; revised 28 February 2022; accepted 1 March 2022; published 14 March 2022)

We studied a mechanism of magnon absorption from a magnon waveguide to adjacent metals. Magnon propagation in the yttrium-iron-garnet magnon waveguide induced/detected via coplanar waveguides was reduced by attaching metals to the magnon waveguide. In particular, the propagating magnon at the surface of the magnon waveguide was largely suppressed by attaching metal strips whereas the uniform or volume mode showed only a very slight decrease. A systematic study on the reduction of magnon propagation was performed by changing the material of metals, changing their thickness, and inserting $SiO_2$ between the magnon waveguide and metals. The reduction in magnon propagation by $SiO_2$ insertion indicated that the eddy-current contribution played a key role in magnon propagation with the magnon gate system with metal electrodes. Our study revealed the relationship between the magnon loss and metallic electrodes, which is indispensable in the fabrication of magnonic devices.

DOI: 10.1103/PhysRevB.105.104415

## I. INTRODUCTION

A magnon is a collective excitation of magnetization in magnetic materials and has been studied as a new information carrier [1–5]. Magnon propagation realizes small-Joule heating propagation and a long propagation length [5], indicating that magnons are promising for low power-consumption information carriers. For example, the propagation length is several millimeters in $Y_3Fe_5O_{12}$ (yttrium-iron-garnet, YIG), which possesses a very low magnetic damping constant and is an insulative material [3,6–10]. For the application of magnons, the magnon-based logic operation was demonstrated via magnon interference and its nonlinearity [5,6,11–13]. These concepts use magnon characteristics as a wave. Recently, the modulation of magnon transport was demonstrated, where magnons are regarded as a form of spin current, spin-wave spin current, and injection/absorption of spin current by an adjacent layer on the magnon waveguide [14–16]. Controlling magnons by considering them as spin current leads to the use of mature manipulation techniques in spintronics.

To realize the modulation of magnon spin current, spin-current injection/absorption layers on the magnon waveguide are required. For example, Das *et al.* [16] demonstrated the modulation of magnon transport by attaching a NiFe alloy (Py) film on a YIG magnon waveguide. Magnons propagate through the YIG magnon waveguide, and their transmission can be controlled by changing the direction of the magnetic moment of Py because the absorption of the spin current into Py can be modulated by the relative angle between the magnetic moment of Py and spin polarization of the spin current. They demonstrated that magnon propagation was significantly reduced when the magnetization of Py and YIG were parallel, indicating that spin-flip scattering and magnon-to-magnon transmission at the Py/YIG interface were the dominant mechanisms of the reduction.

To make further progress in the ferromagnetic-metal gate operation of magnons, increasing the modulation amplitude of the gate operation is required. Here, we consider the ON/OFF state is that magnon can/cannot propagate through the magnon waveguide under the gate electrode, and the modulation amplitude is defined as $N_{ON}$-$N_{OFF}$, where $N_{ON/OFF}$ is the number of magnons detected under the ON/OFF state. One approach to increasing the modulation amplitude of the magnon gate operation is to decrease the absorption of magnons at the ON state where the magnons in the waveguide (YIG) are not absorbed into the gate material (Py). Since Py is a conductive metal and has a large spin-orbit interaction, it is expected to hamper magnon propagation in the ON state via spin-transfer [16], spin-current absorption into adjacent heavy metals [7,9,17–19], or an eddy current in adjacent conductors [20–22] (see Fig. 4(a) in Ref. [16]). Therefore, studying the material dependence of magnon absorption from a magnon waveguide to adjacent metals is quite important. Here, we study magnon absorption from YIG to adjacent ferromagnetic and nonmagnetic middle strips (MSs). We also prepared MSs with a $SiO_2$ insertion layer, which enabled us to study the eddy current contribution to magnon propagation. We found that the surface-propagating magnon was largely suppressed by attaching MS on the YIG waveguide whereas uniform mode (wave number $k = 0$ in the plane of the YIG surface) showed only a very slight decrease. The relationship between the magnon loss and the resistance of MS was inversely proportional, and it can be explained by the generation of the eddy current in MS.

## II. EXPERIMENT

Figure 1 shows the device structure and measurement setup. A 5-$\mu$m YIG film was grown on a (111) gadolinium gallium garnet substrate by liquid-phase epitaxy and was

*These authors contributed equally to this work.
†ohshima.ryo.2x@kyoto-u.ac.jp

 

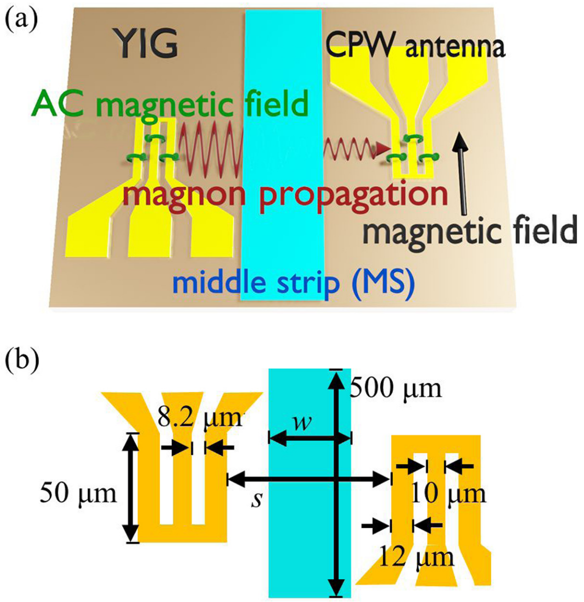


FIG. 1. (a) Schematics of the device structure. CPWs are connected to the vector network analyzer. An external magnetic field $B$ is in the plane of the surface of the YIG and perpendicular to the propagation direction. A MS is fabricated between two CPWs. Magnons are excited by one of the CPWs and detected by the other. During propagation, magnons are absorbed into the MS. (b) Geometry of the device. Thicknesses of MSs, the width of MS $w$, and the distance of two CPWs $s$ are shown in the main text.

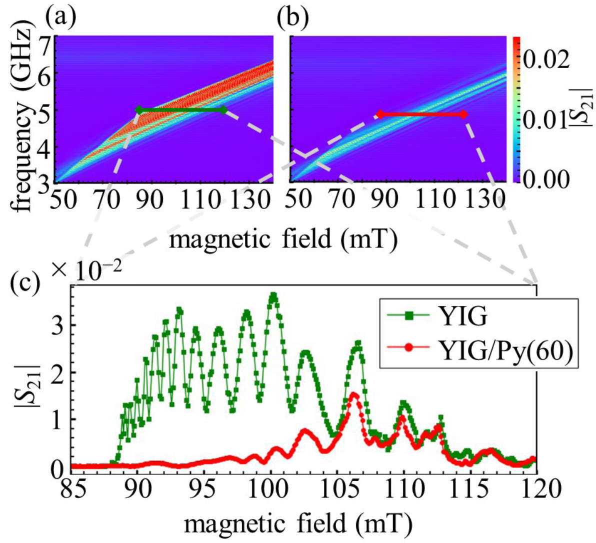


FIG. 2. Color maps of $|S_{21}|$ as a function of $B$ and $f$ for (a) the bare YIG sample and (b) the Py(60)-MS sample. (c) Magnetic field dependence of $|S_{21}|$ at 5 GHz extracted from (a) and (b). A significant decrease in $|S_{21}|$ by attaching 60-nm Py is observed in (b).

commercially available (GRANOPT, Japan). Ti(3 nm)/Au(150 nm) coplanar waveguides (CPWs) and MSs (made of Py, Co, and Pt) were fabricated on YIG by electron-beam (EB) lithography and a subsequent lift-off technique. We used a charge-dissipating agent (ESPACER 300Z, Showa Denko) on the EB lithography resist to avoid charge-up. Py was deposited by EB evaporation and Co and Pt were deposited by rf magnetron sputtering. The thickness of the MSs ranged from 2 to 60 nm, and only Co samples were capped with 2-nm $SiO_2$ protection layers on top. We also prepared devices with $SiO_2$ layers inserted between the MS and the YIG, and their thicknesses ranged from 30 to 100 nm. We prepared samples in various sizes of MSs to check the universality of the magnon-loss effect we observed, and we demonstrated two specific sample geometries in this paper as follows. The distance of the antennas, $s$, and the width of the MS, $w$, were 160 and 100 $\mu$m for devices without inserted $SiO_2$ and 300 and 240 $\mu$m for devices with inserted $SiO_2$, respectively. An in-plane external magnetic field $B$ was applied to the device perpendicular to the magnon propagation direction. The magnetic field was first increased to 180 mT to saturate the magnetization of the YIG and swept from 140 to 50 mT in 0.1-mT decrements. An input AC current with a power of 0 dBm and frequencies from 3 to 7 GHz was injected into the CPW using a vector-network analyzer (VNA) via microwave probes. The AC current generated an induced AC magnetic field in the YIG and excited magnons propagating in the YIG. The magnons were detected by the other CPW as an AC magnetic field by the inverse phenomenon of the excitation of magnons, which was observed as an inductive output voltage. We measured the voltage transmission parameter $S_{21}$ as an index of the number of detected magnons using the VNA. All measurements were carried out at room temperature.

## III. RESULTS AND DISCUSSION

Figures 2(a) and 2(b) show the frequency and magnetic field dependence of $|S_{21}|$ $(=\sqrt{\mathrm{Re}[S_{21}]^2+\mathrm{Im}[S_{21}]^2})$ obtained from the bare YIG sample and the sample with 60-nm Py MS on the YIG [YIG/Py(60)]. Detection of $|S_{21}|$ represents magnon propagation through the YIG substrate. Figure 2(c) shows the external magnetic field dependence of $|S_{21}|$ extracted from Figs. 2(a) and 2(b), with an AC current-frequency of 5 GHz and an external magnetic field from 85 to 120 mT. The intensity of $|S_{21}|$, which reflects the transported magnons, decreases when the Py MS is attached to the YIG. To be more quantitative, we introduce an index of the number of detected magnons, $\Sigma|S_{21}|$, defined by the following equation:

$$\Sigma|S_{21}| = \int_{50\ \mathrm{mT}}^{140\ \mathrm{mT}} |S_{21}(B)|dB. \tag{1}$$

From the result shown in Fig. 2(c), $\Sigma|S_{21}|$ of the bare YIG sample and the YIG/Py(60) sample were estimated to be $4.43\times10^{-3}$ T and $1.20\times10^{-3}$ T, respectively. Thus, $\Sigma|S_{21}|$ was reduced by approximately 73% only by attaching a 60-nm Py MS. Note that $|S_{21}|$ at 5 GHz around the resonance field for the uniform mode ($k=0$), estimated to be 110 mT from the Kittel equation, showed the small attenuation by attaching MS on the channel. On the other hand, $|S_{21}|$ at 5 GHz around the resonance field for the surface mode, estimated to be 95 mT from the magnon dispersion relation and wave vector obtained from the Fourier transform of CPW ($k=0.16\,\mu\mathrm{m}^{-1}$) [23], showed large attenuation [see Fig. 2(c)]. This result indicates that the attenuation of $S_{21}$ was mostly originated from the

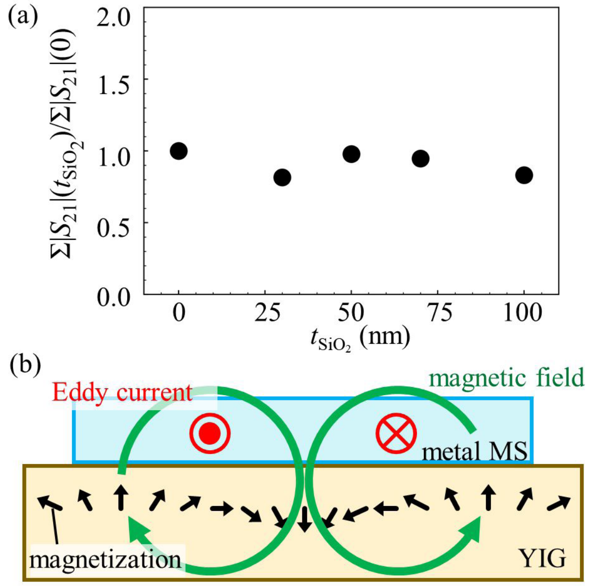


FIG. 3. (a) $SiO_2$ thickness $t_{SiO2}$ dependences of normalized $\Sigma|S_{21}|(t)$ and $\Sigma|S_{21}|(t)/\Sigma|S_{21}|(0)$ for the $YIG/SiO_2(t_{SiO2})/Py(25)$ samples. Data at $t_{SiO2} = 0$ were obtained from samples where YIG and MS were directly connected. The normalized $\Sigma|S_{21}|(t)$ is independent of $t_{SiO2}$. (b) Schematic image of eddy-current generation in the MS from magnon propagation in the YIG.

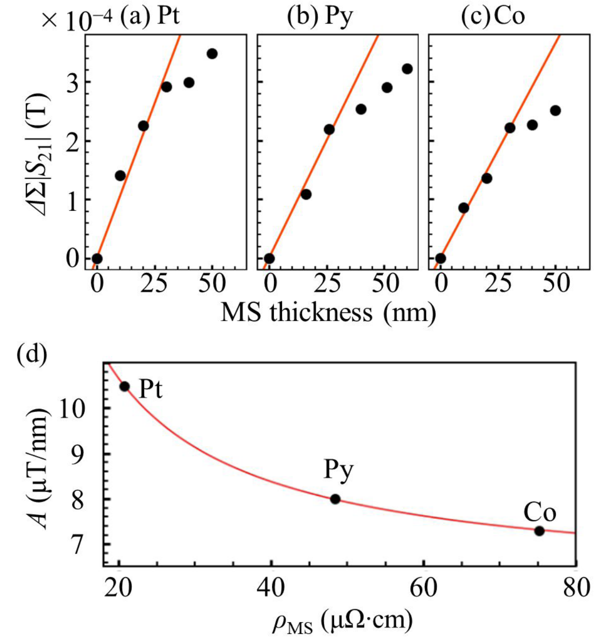


FIG. 4. MS thickness dependences of $\Delta\Sigma|S_{21}| = \Sigma|S_{21}|(0) - \Sigma|S_{21}|(t)$ for the samples with (a) Pt-MS, (b) Py-MS, and (c) Co-MS. $\Sigma|S_{21}|(t)$ is defined in the main text, and data at $t = 0$ nm are obtained from bare YIG samples. The solid red lines are linear fitting of the experimental results in a range that can be considered linear. $\Delta\Sigma|S_{21}|$, indicating magnon loss by attaching MS, monotonically increased with increasing MS thickness. (d) The MS resistivity $\rho_{MS}$ dependence of slope $A$ estimated from the linear fittings of (a)–(c). The red solid line indicates the $A$ inversely proportional to $\rho$.

propagating magnon through the surface of the YIG waveguide.

We investigated the magnon loss with the inserted $SiO_2$ layers. The frequency of the AC current was fixed at 5 GHz in this and all subsequent experiments. Figure 3(a) shows the normalized $\Sigma|S_{21}|$ of $YIG/SiO_2/Py(25)$ with changing $SiO_2$ thickness $t_{SiO2}$. The $SiO_2$ thickness was changed from 30 to 100 nm, and data at $t_{SiO2} = 0$ nm were obtained from the sample where MS and YIG were directly connected. The normalized $\Sigma|S_{21}|$ of $YIG/SiO_2/Py(25)$ was almost constant in all thickness ranges. In a previous study [16], magnon propagation was considered to be suppressed by attaching Py due to magnon-to-magnon scattering, spin-flip scattering, and spin-transfer scattering. As other possible mechanisms, spin-flip scattering and spin-current absorption into adjacent heavy metals via exchange interactions can also be considered because of the large spin interaction of Py [18,19,24–26]. If these mechanisms dominated the magnon loss in our measurement, $\Sigma|S_{21}|$ of the $YIG/SiO_2/Py$ would have increased with increasing $SiO_2$ thickness because the $SiO_2$ insertion layer would have prevented the magnon (spin-current) flow into the Py and the exchange interaction between YIG and Py [27,28] so that the magnon loss (the magnon transmission $\Sigma|S_{21}|$) was suppressed (increased). However, the normalized $\Sigma|S_{21}|$ did not depend on the inserted $SiO_2$ layer between the YIG and MSs or the $SiO_2$ thickness, which indicates that the magnon loss was not related to the mechanisms mentioned above. Here, we propose another possible mechanism for magnon loss: generation of an eddy current in adjacent conductors via magnetization dynamics in the YIG waveguide according to Faraday's law [20–22]. Figure 3(b) shows a schematic image of the generation of the eddy current in adjacent MS. The eddy current can be generated even with the inserted $SiO_2$ layer because its driving force is the inductive magnetic field from the YIG waveguide. Note that only the propagating magnon at the surface of the YIG waveguide was quite sensitive to the adjacent metal strip as shown in Fig. 2(c). The eddy-current contribution in magnon of the uniform and volume modes was considered to be small in thin YIG films because the effect was proportional to the YIG thickness [21]. However, the magnon loss we observed was originated from the surface propagating magnon and it is expected that the magnon loss cannot be ignored even in thin YIG films.

To identify the origin of the magnon loss, we demonstrated the MS thickness dependence of $\Delta\Sigma|S_{21}| = \Sigma|S_{21}|(0) - \Sigma|S_{21}|(t)$, which indicates magnon loss by attaching the MSs (see Fig. 4). Here, the numbers in the brackets indicate the nominal thickness of the layer in nm, and data at $t = 0$ nm were obtained from the bare YIG samples. The magnon loss monotonically increased with increasing MS thickness for each MS. Note that the Pt thickness dependence of the magnon loss was similar to that of Co and Py, indicating that magnon-to-magnon scattering, which was believed to be a factor of magnon loss, cannot explain the MS thickness-dependent magnon loss because magnon propagation is suppressed by attaching both nonmagnetic and ferromagnetic MSs and shows a similar thickness dependence. Since the eddy current was generated according to Faraday's law, this effect is a voltage-induced phenomenon. Thus, the eddy-current contribution appears to be inversely proportional to the MS resistance and proportional to the MS thickness. Note that herein, the $S$ parameters are not power but voltage, so a change in the $S$ parameters can be expressed as being linear to the MS thickness. We also considered the skin depth of MS $\delta$ defined as follows: $\delta = \sqrt{\rho/\pi f \mu}$, where $\rho$ is the resistivity of the metal, $f$ is the microwave frequency, and $\mu$ is the permeability. In our experimental setup, the thickness of metal strips was limited up to 60 nm, which is much thinner than the skin depth of metals at 5 GHz; $\delta$ was estimated to be several micrometers. Therefore, the thick and highly conductive MS generated the eddy current in the MS and screened the stray magnetic field from the YIG waveguide.

In the MS thickness dependence of the magnon loss, the only difference in the MSs that relates to the eddy current is the MS resistivity [20]. Here, we focused on the MSs in small thickness to consider the linear part of the magnon losses. The solid red lines in Figs. 4(a)–4(c) are the linear fitting of the experimental results in a range that can be considered linear, and we can estimate their slope $A$. We also investigated the MS resistivity $\rho_{\mathrm{MS}}$ by the four-terminal measurement and compared it with $A$ [see Fig. 4(d)]. We found a negative correlation between $A$ and $\rho_{\mathrm{MS}}$, and this result is consistent with the magnon loss by the eddy current in MSs; $\Delta\Sigma|S_{21}|$ is inversely proportional to the MS resistance. This result enables us to estimate the magnon loss $\Delta\Sigma|S_{21}|$ of MS with certain thickness and resistivity. The relation can be expressed as follows: $\Delta\Sigma|S_{21}| = At = (b/\rho + c)t$, where $b$ and $c$ are coefficients and we assumed that $t$ is thinner than the skin depth of MS. $c$ is a factor originated from several effects such as the heating of MS or magnon reflection by MS [29], and so on, but independent of the resistivity of MS and does not change in our device structures. To confirm this relationship, we carried out the same measurement with a Cu middle strip (not shown in the text). Since Cu is well conductive ($\rho = 3.53\ \mu\Omega\,\mathrm{cm}$ obtained from the four-terminal measurement), nonlinear behavior appears thinner than other materials, and we used 10-nm Cu-MS. $\Delta\Sigma|S_{21}|$ was estimated to be $2.83 \times 10^{-4}$ T and $3.18 \times 10^{-4}$ T from the experiment and above relationship, respectively, so that the relation obtained from Pt-, Py-, and Co-MSs showed a good agreement with the result in Cu-MS. The influence of the eddy current has not been considered well in the creation of magnon transistors, but we elucidated that the eddy current has a very large impact on magnon propagation under the gating electrode on the magnon waveguide: the generation of an eddy current in the gate electrode strongly hampers magnon propagation at the ON state.

## IV. CONCLUSION

In summary, we studied the impact of attaching metallic middle strips to the YIG magnon waveguide. Magnon propagation was significantly suppressed by attaching both ferromagnetic and nonmagnetic MSs. The magnon loss was not hampered by insertion of the $SiO_2$ layer between the YIG and the MS. Thus, the magnon loss can occur even when there is no direct contact between the YIG and the MS. We also found that the magnon loss monotonically increases with increasing MS thickness. The magnon loss was well expressed by its inverse proportional relationship to the MS resistance, which indicates that the generation of an eddy current in the MS is the dominant magnon-loss mechanism. In particular, the surface-propagating magnon was largely suppressed by attaching MSs whereas the magnon of $k = 0$ in the plane of the YIG surface showed only a very slight decrease. This result indicates that the effect in this study does not decrease with decreasing YIG thickness. The magnon propagation is essential to magnonic devices such as magnon transistors, but it is suppressed by attaching metal electrodes on the waveguide, which is indispensable in the fabrication of magnonic devices. To develop magnonic devices, this effect should be taken into account because any conductors around magnon waveguides can absorb the power of the magnon as an inductive eddy current even without direct contact with the waveguides.

## ACKNOWLEDGMENTS

This work is supported in part by a Grant-in-Aid for Scientific Research (B) (Grant No. 21H01798), Grant-in-Aid for Research Activity Start-up (Grant No. 20K22413), the Murata Science Foundation, Kyoto University Research Development Program (ISHIZUE), and The Kyoto University Foundation.

The authors declare no competing interests.

[1] V. V. Kruglyak and R. J. Hicken, J. Magn. Magn. Mater. **306**, 191 (2006).
[2] V. V. Kruglyak, S. O. Demokritov, and D. Grundler, J. Phys. D: Appl. Phys. **43**, 264001 (2010).
[3] A. A. Serga, A. V. Chumak, and B. Hillebrands, J. Phys. D: Appl. Phys. **43**, 264002 (2010).
[4] B. Lenk, H. Ulrichs, F. Garbs, and M. Münzenberg, Phys. Rep. **507**, 107 (2011).
[5] A. V. Chumak, V. I. Vasyuchka, A. A. Serga, and B. Hillebrands, Nat. Phys. **11**, 453 (2015).
[6] T. Schneider, A. A. Serga, B. Leven, B. Hillebrands, R. L. Stamps, and M. P. Kostylev, Appl. Phys. Lett. **92**, 022505 (2008).
[7] Y. Kajiwara, K. Harii, S. Takahashi, J. Ohe, K. Uchida, M. Mizuguchi, H. Umezawa, H. Kawai, K. Ando, K. Takanashi, S. Maekawa, and E. Saitoh, Nature (London) **464**, 262 (2010).
[8] H. Yu, O. d'Allivy Kelly, V. Cros, R. Bernard, P. Bortolotti, A. Anane, F. Brandl, R. Huber, I. Stasinopoulos, and D. Grundler, Sci. Rep. **4**, 6848 (2015).
[9] L. J. Cornelissen, J. Liu, R. A. Duine, J. B. Youssef, and B. J. van Wees, Nat. Phys. **11**, 1022 (2015).
[10] C. Dubs, O. Surzhenko, R. Linke, A. Danilewsky, U. Brückner, and J. Dellith, J. Phys. D: Appl. Phys. **50**, 204005 (2017).
[11] K.-S. Lee and S.-K. Kim, J. Appl. Phys. **104**, 053909 (2008).
[12] A. V. Chumak, A. A. Serga, and B. Hillebrands, Nat. Commun. **5**, 4700 (2014).

[13] A. V. Chumak, V. I. Vasyuchka, A. A. Serga, M. P. Kostylev, V. S. Tiberkevich, and B. Hillebrands, Phys. Rev. Lett. **108**, 257207 (2012).
[14] L. J. Cornelissen, J. Liu, B. J. van Wees, and R. A. Duine, Phys. Rev. Lett. **120**, 097702 (2018).
[15] A. Navabi, Y. Liu, P. Upadhyaya, K. Murata, F. Ebrahimi, G. Yu, B. Ma, Y. Rao, M. Yazdani, M. Montazeri, L. Pan, I. N. Krivorotov, I. Barsukov, Q. Yang, P. Khalili Amiri, Y. Tserkovnyak, and K. L. Wang, Phys. Rev. Appl. **11**, 034046 (2019).
[16] K. S. Das, F. Feringa, M. Middelkamp, B. J. van Wees, and I. J. Vera-Marun, Phys. Rev. B **101**, 054436 (2020).
[17] A. V. Chumak, A. A. Serga, M. B. Jungfleisch, R. Neb, D. A. Bozhko, V. S. Tiberkevich, and B. Hillebrands, Appl. Phys. Lett. **100**, 082405 (2012).
[18] K. S. Das, W. Y. Schoemaker, B. J. van Wees, and I. J. Vera-Marun, Phys. Rev. B **96**, 220408(R) (2017).
[19] K. S. Das, J. Liu, B. J. van Wees, and I. J. Vera-Marun, Nano Lett. **18**, 5633 (2018).
[20] M. A. W. Schoen, J. M. Shaw, H. T. Nembach, M. Weiler, and T. J. Silva, Phys. Rev. B **92**, 184417 (2015).
[21] S. A. Bunyaev, R. O. Serha, H. Yu. Musiienko-Shmarova, A. J. E. Kreil, P. Frey, D. A. Bozhko, V. I. Vasyuchka, R. V. Verba, M. Kostylev, B. Hillebrands, G. N. Kakazei, and A. A. Serga, Phys. Rev. Appl. **14**, 024094 (2020).
[22] D. A. Bozhko, A. A. Serga, M. Agrawal, B. Hillebrands, and M. P. Kostylev, arXiv:1603.09201.
[23] V. Vlaminck and M. Bailleul, Phys. Rev. B **81**, 014425 (2010).
[24] B. F. Miao, S. Y. Huang, D. Qu, and C. L. Chien, Phys. Rev. Lett. **111**, 066602 (2013).
[25] A. Tsukahara, Y. Ando, Y. Kitamura, H. Emoto, E. Shikoh, M. P. Delmo, T. Shinjo, and M. Shiraishi, Phys. Rev. B **89**, 235317 (2014).
[26] Y. Omori, E. Sagasta, Y. Niimi, M. Gradhand, L. E. Hueso, F. Casanova, and Y. Otani, Phys. Rev. B **99**, 014403 (2019).
[27] O. Mosendz, J. E. Pearson, F. Y. Fradin, S. D. Bader, and A. Hoffmann, Appl. Phys. Lett. **96**, 022502 (2010).
[28] C. H. Du, H. L. Wang, Y. Pu, T. L. Meyer, P. M. Woodward, F. Y. Yang, and P. C. Hammel, Phys. Rev. Lett. **111**, 247202 (2013).
[29] N. Guan, K. Yashiro, and S. Ohkawa, An integral kernel expansion approach to analysis of reflection of magnetostatic surface waves by a microstrip, in *Proceedings of 1993 Asia Pacific Microwave Conference (APMC'93)* (IEEE, 1993), p. 10, doi: 10.1109/APMC.1993.468659.